
Nanofluid flow and heat transfer over a stretching porous cylinder considering thermal radiation

M. Sheikholeslami¹, M. T. Mustafa² and D. D. Ganji^{1*}

¹*Department of Mechanical Engineering, Babol University of Technology, Babol, Islamic Republic of Iran*

²*Department of Mathematics, Statistics and Physics, Qatar University, Doha 2713, Qatar*

E-mail: mohsen.sheikholeslami@yahoo.com, m_sh_3750@yahoo.com & ddg_davood@yahoo.com

Abstract

The aim of the present paper is to study the Cu-water nanofluid flow and heat transfer characteristics of a stretching permeable cylinder. Thermal radiation effect is considered in energy equation. The governing partial differential equations with the corresponding boundary conditions are reduced to a set of ordinary differential equations with the appropriate boundary conditions using similarity transformation, which is then solved numerically by the fourth order Runge–Kutta integration scheme featuring a shooting technique. Numerical results for the flow and heat transfer characteristics are obtained for various values of the nanoparticle volume fraction, suction parameter, Reynolds number and radiation parameter. The results show that skin friction coefficient increases with increase of Reynolds number and suction parameter but it decreases with increase of nanoparticle volume fraction. Nusselt number is an increasing function of nanoparticle volume fraction, Reynolds number and suction parameter but it is a decreasing function of radiation parameter.

Keywords: Thermal radiation; nanofluid; boundary layer; stretching cylinder; heat transfer; porous media

1. Introduction

The study of convective heat transfer in fluid-saturated porous media has many important applications in technology of geothermal energy recovery such as oil recovery, food processing, fiber and granular insulation, porous burner and heater, combustion of low-calorific fuels to diesel engines and design of packed bed reactors. In general, suction tends to increase the skin friction and heat transfer coefficients, whereas injection acts in the opposite manner. The effects of suction/injection on the flow and heat transfer over a slender cylinder are of practical interest and have attracted many researchers to make further investigations. (Ishak et al., 2008) studied uniform suction/blowing effect on flow and heat transfer due to a stretching cylinder that is useful as a simple model in understanding more complicated applications to practical problems, such as cooling of nuclear reactors.

Steady flow in a viscous and incompressible fluid outside of a stretching hollow cylinder in an ambient fluid at rest has been done by (Wang, 1988). The problem is governed by a third-order nonlinear ordinary differential equation that leads to

exact similarity solutions of the Navier–Stokes equations. Flow over cylinder is considered to be two-dimensional if the body radius is large compared to the boundary layer thickness. On the other hand, for a thin or slender cylinder, the radius of the cylinder may be of the same order as that of the boundary layer thickness.

The thermal radiation has a significant role in the overall surface heat transfer when the convection heat transfer coefficient is small. (Hayat et al., 2010a) studied the effects of radiation and magnetic field on the mixed convection stagnation-point flow over a vertical stretching sheet in a porous medium. They found that the values of skin friction coefficient and the local Nusselt number are tabulated in both cases of assisting and opposing flows. Effect of thermal radiation and Joule heating on MHD flow of a Maxwell fluid in the presence of thermophoresis is investigated by (Hayat et al., 2010b). Thermal analysis of the mixed convection-radiation of an inclined flat plate embedded in a porous medium was conducted by (Moradi et al., 2013).

Recently, due to the rising demands of modern technology, including chemical production, power station, and microelectronics, there is a need to develop new types of fluids that will be more effective in terms of heat exchange performance. Nanofluids are produced by dispersing the nanometer-scale solid particles into base liquids

*Corresponding author

Received: 25 July 2013 / Accepted: 27 January 2015

with low thermal conductivity such as water, ethylene glycol (EG), oils, etc. The term “nanofluid” was first coined by (Choi, 1995) to describe this new class of fluids. The materials with sizes of nanometers possess unique physical and chemical properties. The presence of the nanoparticles in the fluids noticeably increases the effective thermal conductivity of the fluid and consequently enhances the heat transfer characteristics. Therefore, numerous methods have been taken to improve the thermal conductivity of these fluids by suspending nano/micro-sized particle materials in liquids.

MHD effect on natural convection heat transfer in an inclined L-shape enclosure filled with nanofluid was studied by (Sheikholeslami et al., 2014a). They found that enhancement in heat transfer has reverse relationship with Hartmann number and Rayleigh number. (Rashidi et al., 2013) considered the analysis of the second law of thermodynamics applied to an electrically conducting incompressible nanofluid fluid flowing over a porous rotating disk. They concluded that using magnetic rotating disk drives has important applications in heat transfer enhancement in renewable energy systems. (Sheikholeslami et al., 2013a) used heatline analysis to simulate two phase simulation of nanofluid flow and heat transfer. Their results indicated that the average Nusselt number decreases as buoyancy ratio number increases until it reaches a minimum value and then starts increasing. (Sheikholeslami et al., 2014b) analyzed the magnetohydrodynamic nanofluid flow and heat transfer between two horizontal plates in a rotating system. Their results indicated that, for both suction and injection Nusselt number has a direct relationship with nanoparticle volume fraction. Nanofluid flow and heat transfer has been investigated by several authors (Sheikholeslami et al., 2013(b,c,d), Sheikholeslami et al., 2012, Hayat et al., 2012 (a,b), Sheikholeslami et al., 2014(c,d), Shehzad et al., 2012, Sheikholeslami and Gorji-Bandpy, 2014, Shehzad et al., 2013a, Sheikholeslami and Ganji, 2014 (a,b,c). Effect of magnetic field on nanofluid flow and heat transfer has been considered by different authors (Sheikholeslami et al., 2014(e, f, g, h, i), Shehzad et al., 2013b, Sheikholeslami and Ganji, 2014 (d,e), Hayat et al., 2007, Sheikholeslami et al., 2013e, Hayat et al., 2014, Shehzad et al., 2014 (a,b), Sheikholeslami et al., 2015(a, b)).

The objective of the present paper is to study the nanofluid flow and heat transfer due to a stretching cylinder with uniform suction. Thermal radiation is taken in to account. The reduced ordinary differential equations are solved numerically using the fourth order Runge–Kutta integration scheme featuring a shooting technique. The effects of the

parameters governing the problem are studied and discussed.

2. Problem formulation

Consider the steady laminar flow of an incompressible nanofluid caused by a stretching tube with radius a in the axial direction in a fluid at rest as shown in Fig. 1, where the z -axis is measured along the axis of the tube and the r -axis is measured in the radial direction. It is assumed that the surface of the tube is at constant temperature T_w and the ambient fluid temperature is T_∞ where $T_w > T_\infty$. The viscous dissipation is neglected as it is assumed to be small. It is assumed that the base fluid and the nanoparticles are in thermal equilibrium and no slip occurs between them. The thermo physical properties of the nanofluid are given in Table1.

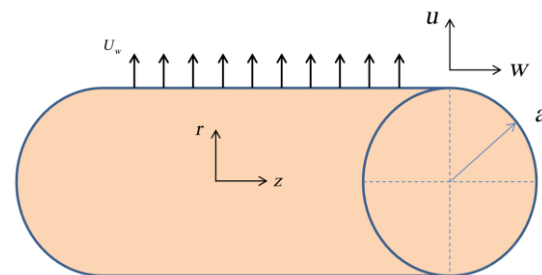


Fig. 1. Figure of geometry

Table1. Thermo physical properties of water and nanoparticles

	$\rho(\text{kg} / \text{m}^3)$	$C_p(\text{J} / \text{kgK})$	$k(\text{W} / \text{mK})$
water	997.1	4179	0.613
Cu	8933	385	401

Under these assumptions, the governing equations are

$$\frac{\partial(nw)}{\partial z} + \frac{\partial(mu)}{\partial r} = 0, \quad (1)$$

$$\rho_{nf} \left(w \frac{\partial w}{\partial z} + u \frac{\partial w}{\partial r} \right) = \mu_{nf} \left(\frac{\partial^2 w}{\partial r^2} + \frac{1}{r} \frac{\partial w}{\partial r} \right), \quad (2)$$

$$\rho_{nf} \left(w \frac{\partial u}{\partial z} + u \frac{\partial u}{\partial r} \right) = -\frac{\partial P}{\partial r} + \mu_{nf} \left(\frac{\partial^2 u}{\partial r^2} + \frac{1}{r} \frac{\partial u}{\partial r} - \frac{u}{r^2} \right), \quad (3)$$

$$\left(w \frac{\partial T}{\partial z} + u \frac{\partial T}{\partial r} \right) = \frac{k_{nf}}{(\rho C_p)_{nf}} \left(\frac{\partial^2 T}{\partial r^2} + \frac{1}{r} \frac{\partial T}{\partial r} \right) - \frac{\partial q_r}{\partial r}, \quad (4)$$

where the radiation heat flux q_r is considered according to Rosseland approximation such that

$$q_r = -\frac{4\sigma_e}{3\beta_R} \frac{\partial T^4}{\partial y} \text{ where } \sigma_e, \beta_R \text{ are the Stefan–Boltzmann}$$

constant and the mean absorption coefficient, respectively. Following (Raptis, 1998), the fluid-phase temperature differences within the flow are assumed to be sufficiently small so that T^4 may be expressed as a linear function of temperature. This is done by expanding T^4 in a Taylor series about the temperature T_∞ and neglecting higher order terms to yield $T^4 \cong 4T_\infty^3 T - 3T_\infty^4$.

The boundary conditions are:

$$\begin{aligned} r=a & : u=U_w, \quad w=w_w, \quad T=T_w \\ r \rightarrow \infty & : w \rightarrow 0, \quad T \rightarrow T_\infty \end{aligned} \tag{5}$$

where $U_w = -ca\gamma$, $w_w = 2cz$ and c is a positive constant. Notice that γ is a constant in which $\gamma > 0$ and $\gamma < 0$ correspond to mass suction and mass injection, respectively. The effective density ρ_{nf} , the effective dynamic viscosity μ_{nf} , the heat capacitance $(\rho C_p)_{nf}$ and the thermal conductivity k_{nf} of the nanofluid are given as (Khanafar et al., 2003):

$$\rho_{nf} = \rho_f(1-\phi) + \rho_s\phi \tag{6}$$

$$\mu_{nf} = \frac{\mu_f}{(1-\phi)^{2.5}} \tag{7}$$

$$(\rho C_p)_{nf} = (\rho C_p)_f(1-\phi) + (\rho C_p)_s\phi \tag{8}$$

$$\frac{k_{nf}}{k_f} = \frac{k_s + (n-1)k_f - (n-1)\phi(k_f - k_s)}{k_s + (n-1)k_f + \phi(k_f - k_s)} \tag{9}$$

Here, ϕ is the nanoparticle volume fraction. Following (Wang, 1988) we take the similarity transformation:

$$\begin{aligned} \eta &= (r/a)^2, & u &= -ca[f(\eta)/\sqrt{\eta}], \\ w &= 2cf'(\eta)z, & \theta(\eta) &= (T - T_\infty)/(T_w - T_\infty), \end{aligned} \tag{10}$$

where prime denotes differentiation with respect to η . Substituting Eq. (10) into Eqs. (2) and (4), we get the following ordinary differential equations:

$$Re A_1 (1-\phi)^{2.5} (f'^2 - ff'') = \eta f''' + f''', \tag{11}$$

$$\left(\eta + \frac{4 Rd}{3 A_3} \right) \theta'' + (1 + Re Pr_f A_2 / A_3) \theta' = 0, \tag{12}$$

where $Re = ca^2 / 2\nu_f$ is the Reynolds number, $\nu_f = \mu_f / \rho_f$ the kinematic viscosity, $Pr = \mu_f (\rho C_p)_f / (\rho_f k_f)$ is the Prandtl number, $Rd = 4\sigma_e T_\infty^3 / (\beta_R k_f)$ is Radiation parameter and A_1, A_2, A_3 are parameters having the following forms:

$$A_1 = (1-\phi) + \frac{\rho_s}{\rho_f} \phi \tag{13}$$

$$A_2 = (1-\phi) + \frac{(\rho C_p)_s}{(\rho C_p)_f} \phi \tag{14}$$

$$A_3 = \frac{k_{nf}}{k_f} = \frac{k_s + 2k_f - 2\phi(k_f - k_s)}{k_s + 2k_f + \phi(k_f - k_s)} \tag{15}$$

The boundary conditions (5) become

$$\begin{aligned} f(1) &= \gamma, \quad f'(1) = 1, \quad \theta(1) = 1, \\ f'(\infty) &\rightarrow 0, \quad \theta(\infty) \rightarrow 0. \end{aligned} \tag{16}$$

The pressure (P) can now be determined from Eq. (3) in the form

$$\frac{P}{\rho_{nf}} = \frac{P_\infty}{\rho_{nf}} - \frac{c^2 a^2}{2\eta} f'^2(\eta) - 2c \nu_{nf} f'(\eta), \tag{17}$$

$$\frac{P - P_\infty}{\rho_{nf} c \nu_{nf}} = -\frac{Re}{\eta} A_1 (1-\phi)^{2.5} f'^2(\eta) - 2f'(\eta). \tag{18}$$

Physical quantities of interest are the skin friction coefficient (C_f) and the Nusselt number (Nu), which are defined as

$$\tau_w = \mu_{nf} \left(\frac{\partial w}{\partial r} \right)_{r=a} \tag{20a}$$

$$q_w = -k_{nf} \left(\frac{\partial T}{\partial r} \right)_{r=a} \tag{20b}$$

i.e.

$$\tau_w = \frac{4\mu_{nf} c z}{a} f''(1) \tag{21a}$$

$$q_w = -\frac{2k_{nf} (T_w - T_\infty)}{a} \theta'(1) \tag{21b}$$

Using variables (10), we have:

$$C_f (Re z / a) = \frac{1}{A_1 (1-\phi)^{2.5}} f''(1) \tag{22a}$$

$$Nu = -2 \frac{k_{nf}}{k_f} \theta'(1) \tag{22b}$$

3. Numerical method

Before employing the Runge-Kutta integration scheme, first we reduce the governing differential equations into a set of first order ODEs. Let $x_1 = \eta, x_2 = f, x_3 = f', x_4 = f'', x_5 = \theta, x_6 = \theta'$. We obtain the following system:

$$\begin{pmatrix} x_1' \\ x_2' \\ x_3' \\ x_4' \\ x_5' \\ x_6' \end{pmatrix} = \begin{pmatrix} 1 \\ x_3 \\ x_4 \\ \left[\text{Re}A_1(1-\phi)^{2.5}(x_3^2-x_4x_2)-x_4 \right] / \eta \\ x_6 \\ x_7 \\ -(1+\text{Re}Prx_2A_2/A_3)x_7 / (\eta+4Rd / (3A_3)) \end{pmatrix} \quad (23)$$

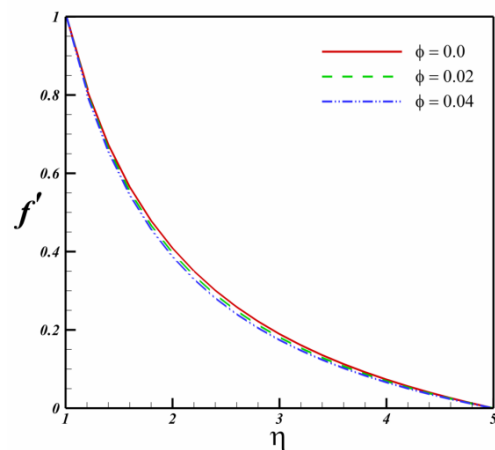
and the corresponding initial conditions are

$$\begin{pmatrix} x_1 \\ x_2 \\ x_3 \\ x_4 \\ x_5 \\ x_6 \end{pmatrix} = \begin{pmatrix} 1 \\ \gamma \\ 1 \\ u_1 \\ 1 \\ u_2 \end{pmatrix} \quad (24)$$

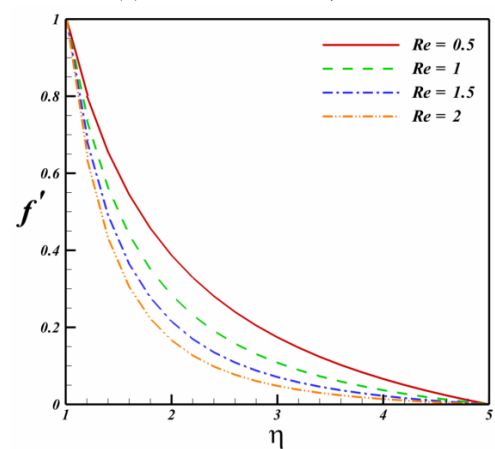
The above nonlinear coupled ODEs along with initial conditions are solved using fourth Order Runge-Kutta integration technique. Suitable values of the unknown initial conditions u_1 and u_2 are approximated through Newton's method until the boundary conditions at $f'(\infty) \rightarrow 0, \theta(\infty) \rightarrow 0$ are satisfied. The computations have been performed by using MAPLE. The maximum value of $\eta = \infty$, to each group of parameters is determined when the values of unknown boundary conditions at $x = 1$ do not change to a successful loop with error less than 10^{-6} .

4. Results and discussion

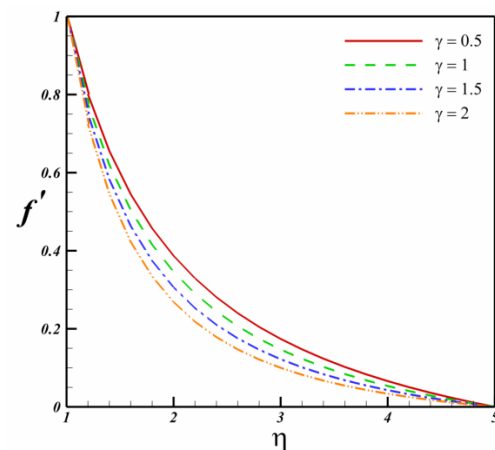
Effect of thermal radiation on Cu-water nanofluid hydrothermal behavior over a cylinder is studied. The governing equations and their boundary conditions are transformed to ordinary differential equations which are solved numerically using the fourth order Runge-Kutta integration scheme featuring a shooting technique. Table 1 shows thermo physical properties of water and Cu nanoparticle. In order to test the accuracy of the present results, we have compared the results for $-\theta(1)$ with those of (Ishak et al., 2008 and Wang, 1988), when $\phi=0$ (classical viscous fluid). We notice that the comparison shows an excellent agreement, as presented in Table 2. Fig. 2 shows the effects of nanoparticle volume fraction, Reynolds number and suction parameter on velocity profile. The momentum boundary layer thickness decreases with increase of nanoparticle volume fraction. Effects of Reynolds number and suction parameter on momentum boundary layer thickness are similar to that of nanoparticle volume fraction.



(a) $Re = 0.5, Rd = 0.5, \phi = 0.04$



(b) $Rd = 0.5, \phi = 0.04, \gamma = 0.5$



(c) $Re = 0.5, Rd = 0.5, \phi = 0.04$

Fig. 2. Effects of nanoparticle volume fraction, Reynolds number and suction parameter on velocity profile when $Pr = 7$

Table 2. Compared the results for $-\theta'(1)$ with those of Ishak et al. (2008) and Wang (1988), when $\varphi=0$ (classical viscous fluid), for several values of M , Pr when $Re=10$

Pr	M	Ishak et al. (2008)	Wang (1988)	Present study
0.7	0	1.5687	1.568	1.564442
0.7	0.05	1.5665		1.562785
0.7	0.5	1.5478		1.548292
0.7	2	1.4924		1.504783
0.7	5	1.4012		1.43423
7	0	6.1592	6.16	6.157509
7	0.05	6.1573		6.155608
7	0.5	6.1402		6.138764
7	2	6.0864		6.085643
7	5	5.9855		5.989984

Effects of nanoparticle volume fraction, Reynolds number and suction parameter on skin friction coefficient are shown in Fig. 3. Skin friction coefficient has direct relationship with Reynolds number and suction parameter while it has the rever relationship with nanoparticle volume fraction. Fig. 4 shows the effects of Reynolds number and suction parameter on pressure distribution. Pressure distribution decreases with increase of Reynolds number and suction parameter.

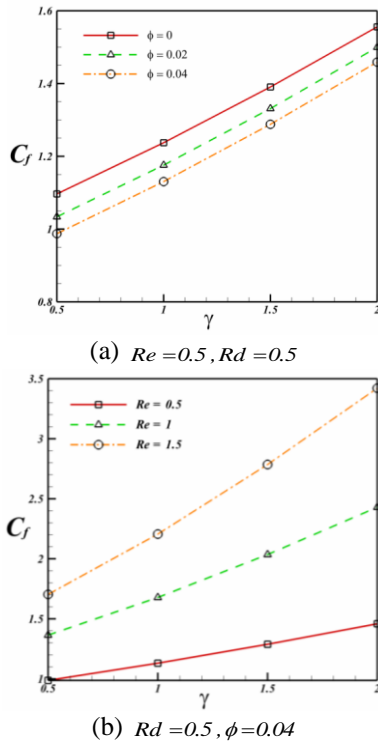


Fig. 3. Effects of nanoparticle volume fraction, Reynolds number and suction parameter on skin friction coefficient when $Pr=7$

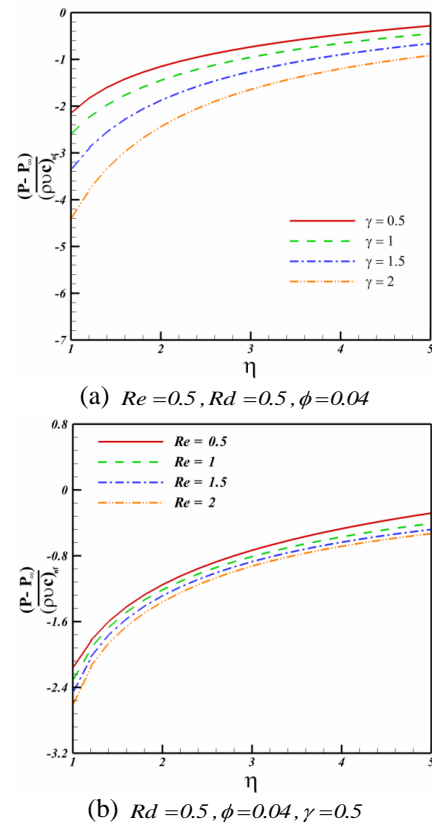
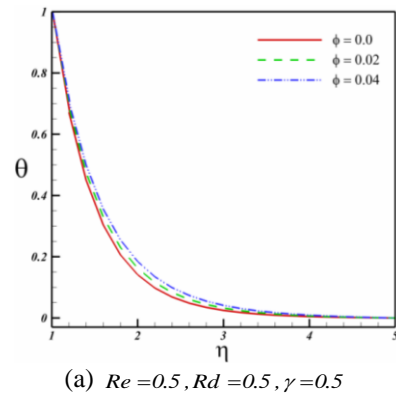


Fig. 4. Effects of Reynolds number and suction parameter on pressure distribution when $Pr=7$

Fig. 5 shows the effects of nanoparticle volume fraction, Reynolds number, suction parameter and radiation parameter on temperature profile. Thermal boundary layer thickness decreases with increase of Reynolds number, suction parameter while it increases with increase of nanoparticle volume fraction and radiation parameter. Fig. 6 shows the effects of nanoparticle volume fraction, Reynolds number, suction parameter and radiation parameter on Nusselt number. Nusselt number has direct relationship with nanoparticle volume fraction, Reynolds number, suction parameter and it has a rever relationship with radiation parameter.



(a) $Re=0.5, Rd=0.5, \gamma=0.5$

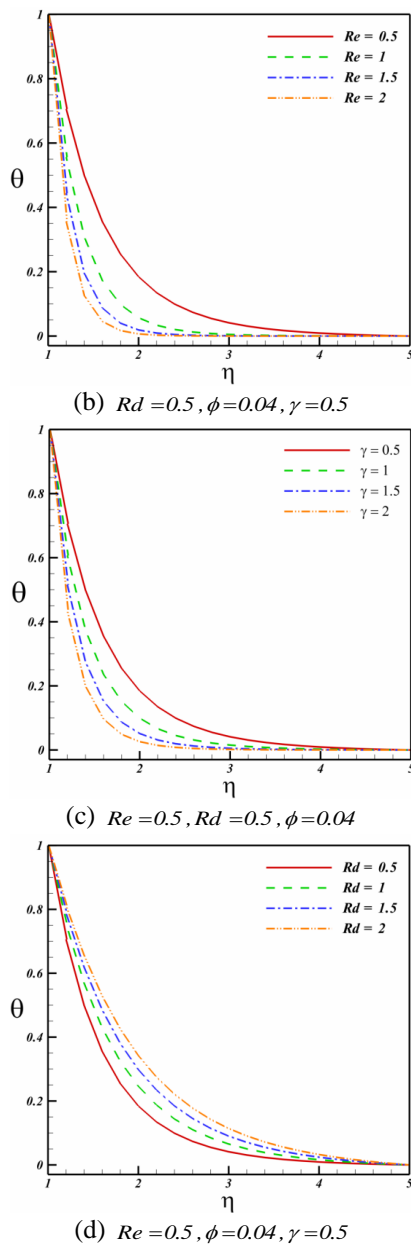


Fig. 5. Effects of nanoparticle volume fraction, Reynolds number, suction parameter and radiation parameter on temperature profile when $Pr = 7$

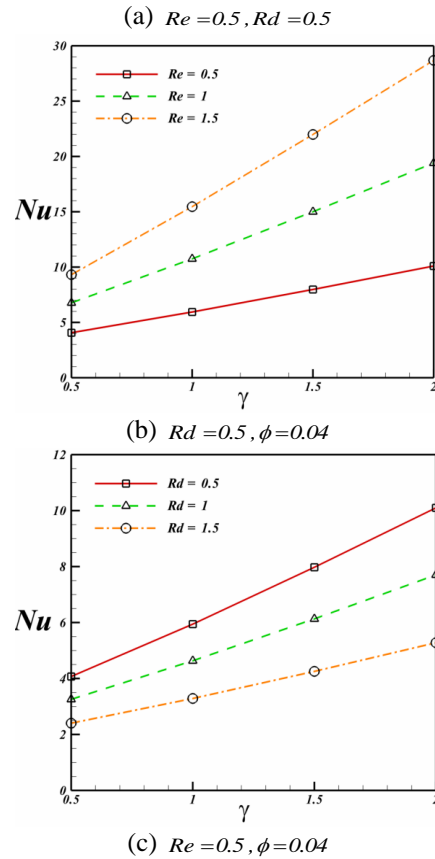
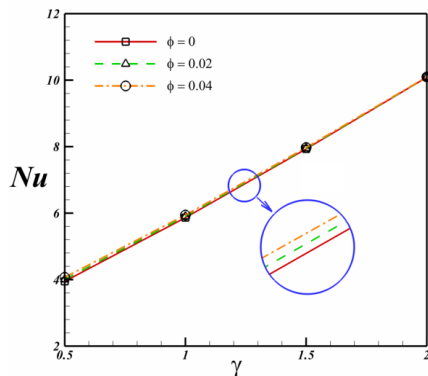


Fig. 6. Effects of nanoparticle volume fraction, Reynolds number, suction parameter and radiation parameter on Nusselt number when $Pr = 7$

5. Conclusions

The steady two-dimensional nanofluid flow due to a stretching permeable tube has been investigated. Thermal radiation effect is considered in this study. The equations are solved numerically using the fourth-order Runge–Kutta method. Effects of nanoparticle volume fraction, suction parameter, Reynolds number and radiation parameter on the flow and heat transfer characteristics have been examined. Axial velocity decreases with increase of Temperature profile increases with increase of nanoparticle volume fraction and radiation parameter while it decreases with increase of suction parameter and Reynolds number.

References

Choi, S. U. S. (1995). Enhancing Thermal Conductivity of Fluids with Nanoparticles. *The Proceedings of the 1995 ASME International Mechanical Engineering Congress and Exposition, San Francisco, USA, ASME, FED 231/MD*, 66, 99–105.

Das, S. K., Choi, S. U. S., Yu, W., & Pradeep, T. (2007). *Nanofluids. Science and Technology*, Wiley, New Jersey.

- Hayat, T., Abbas, Z., Pop, I., & Asghar, S. (2010). Effects of radiation and magnetic field on the mixed convection stagnation-point flow over a vertical stretching sheet in a porous medium. *International Journal of Heat and Mass Transfer*, 53, 466–474.
- Hayat, T., & Qasim, M. (2010). Influence of thermal radiation and Joule heating on MHD flow of a Maxwell fluid in the presence of thermophoresis. *International Journal of Heat and Mass Transfer*, 53, 4780–4788.
- Hayat, T., Ahmed, N., Sajid, M., & Asghar, S. (2007). On the MHD flow of a second grade fluid in a porous channel. *Computers & Mathematics with Applications*, 54(3), 407–414.
- Hayat, T., Shehzad, S. A., Qasim, M., & Obaidat, S. (2012a). Radiative flow of Jeffery fluid in a porous medium with power law heat flux and heat source. *Nuclear Engineering and Design*, 243, 15–19.
- Hayat, T., Shehzad, S. A., & Alsaedi, A. (2012b). Soret and Dufour effects in magnetohydrodynamic (MHD) flow of Casson fluid. *Applied Mathematics and Mechanics-English Edition*, 33, 1301–1312.
- Hayat, T., Abbasi, F. M., Al-Yami, M., & Monaque, S. (2014). Slip and Joule heating effects in mixed convection peristaltic transport of nanofluid with Soret and Dufour effects. *Journal of Molecular Liquids*, 194, 93–99.
- Ishak, A., Nazar, R., & Pop, I. (2008). Uniform suction/blowing effect on flow and heat transfer due to a stretching cylinder. *Applied Mathematical Modelling*, 32, 2059–2066.
- Wang, C. Y. (1988). Fluid flow due to a stretching cylinder. *Phys. Fluids*, 31, 466–468.
- Khanafar, K., Vafai K., & Lightstone M. (2003). Buoyancy-driven heat transfer enhancement in a two-dimensional enclosure utilizing nanofluids. *International Journal of Heat and Mass Transfer*, 446, 3639–3653.
- Moradi, A., Ahmadikia, H., Hayat, T., & Alsaedi, A. (2013). On mixed convection-radiation interaction about an inclined plate through a porous medium. *International Journal of Thermal Sciences*, 64, 129–136.
- Raptis A. (1998). Radiation and free convection flow through a porous medium. *Int. Commun. HeatMass Transfer*, 25, 289–295.
- Sheikholeslami, M., Gorji-Bandpay, M., & Ganji, D. D. (2012). Magnetic field effects on natural convection around a horizontal circular cylinder inside a square enclosure filled with nanofluid. *International Communications in Heat and Mass Transfer*, 39, 978–986.
- Sheikholeslami, M., Gorji-Bandpy, M., & Soleimani, S. (2013a). Two phase simulation of nanofluid flow and heat transfer using heatline analysis. *International Communications in Heat and Mass Transfer*, 47, 73–81.
- Sheikholeslami, M., & Ganji, D. D. (2013b). Heat transfer of Cu-water nanofluid flow between parallel plates. *Powder Technology*, 235, 873–879.
- Sheikholeslami, M., Gorji-Bandpy, M., & Ganji, D. D. (2013c). Numerical investigation of MHD effects on Al₂O₃-water nanofluid flow and heat transfer in a semi-annulus enclosure using LBM. *Energy*, 60, 501–510.
- Sheikholeslami, M., Gorji-Bandpy, M., & Domairry, G. (2013d). Free convection of nanofluid filled enclosure using lattice Boltzmann method (LBM). *Appl. Math. Mech. Engl. Ed.*, 34(7), 1–15.
- Shehzad, S. A., Alsaedi, A., & Hayat, T. (2012). Three-dimensional flow of Jeffery fluid with convective surface boundary conditions. *International Journal of Heat and Mass Transfer*, 55, 3971–3976.
- Shehzad, S. A., Hayat, T., Qasim, M., & Asghar, S. (2013a). Effects of mass transfer on MHD flow of Casson fluid with chemical reaction and suction. *Brazilian Journal of Chemical Engineering*, 30, 187–195.
- Shehzad, S. A., Qasim, M., Alsaedi, A., Hayat, T., & Alhuthali, M. S. (2013b). Combined effects of thermal stratification and thermal radiation in mixed convection flow of thixotropic fluid. *The European Physical Journal Plus*, 128, 1–7.
- Shehzad, S. A., Alsaedi, A., Hayat, T., & Alhuthali, M. S. (2014a). Thermophoresis particle deposition in mixed convection three-dimensional radiative flow of an Oldroyd-B fluid. *Journal of the Taiwan Institute of Chemical Engineers*, 45, 787–794.
- Shehzad, S. A., Alsaedi, F. E., Hayat, T., & Monaque, S. J. (2014b). MHD mixed convection flow of thixotropic fluid with thermal radiation. *Heat Transfer Research*, 45, 659–676.
- Sheikholeslami, M., Gorji-Bandpy, M., & Ganji, D. D. (2013e). Natural convection in a nanofluid filled concentric annulus between an outer square cylinder and an inner elliptic cylinder. *Scientia Iranica, Transaction B: Mechanical Engineering*, 20(4), 1241–1253.
- Sheikholeslami, M., Ganji, D. D., Gorji-Bandpy, M., & Soleimani, S. (2014a). Magnetic field effect on nanofluid flow and heat transfer using KKL model. *Journal of the Taiwan Institute of Chemical Engineers*, 45, 795–807.
- Sheikholeslami, M., Hatami, M., & Ganji, D. D. (2014b). Nanofluid flow and heat transfer in a rotating system in the presence of a magnetic field. *Journal of Molecular Liquids*, 190, 112–120.
- Sheikholeslami, M., Gorji-Bandpy, M., Ganji, D. D., Rana, P., & Soleimani, S. (2014c). Magnetohydrodynamic free convection of Al₂O₃-water nanofluid considering Thermophoresis and Brownian motion effects. *Computers & Fluids*, 94, 147–160.
- Sheikholeslami, M., Gorji-Bandpy, M., & Ganji, D. D. (2014d). Lattice Boltzmann method for MHD natural convection heat transfer using nanofluid. *Powder Technology*, 254, 82–93.
- Sheikholeslami, M., Gorji Bandpy, M., Ellahi, R., & Zeeshan, A. (2014e). Simulation of MHD CuO–water nanofluid flow and convective heat transfer considering Lorentz forces. *Journal of Magnetism and Magnetic Materials*, 369, 69–80.
- Sheikholeslami, M., Gorji-Bandpy, M., & Ganji, D. D. (2014f). MHD free convection in an eccentric semi-annulus filled with nanofluid. *Journal of the Taiwan Institute of Chemical Engineers*, 45, 1204–1216.
- Sheikholeslami, M., Gorji-Bandpy, M., Ganji, D. D., & Soleimani, S. (2014g). Natural convection heat transfer

- in a cavity with sinusoidal wall filled with CuO-water nanofluid in presence of magnetic field. *Journal of the Taiwan Institute of Chemical Engineers*, 45, 40–49.
- Sheikholeslami, M., Gorji-Bandpay, M., & Ganji, D. D. (2014h). Investigation of nanofluid flow and heat transfer in presence of magnetic field using KKL model. *Arabian Journal for Science and Engineering*, 39(6), 5007–5016.
- Sheikholeslami, M., Abelman, S., & Ganji, D. D. (2014 i). Numerical simulation of MHD nanofluid flow and heat transfer considering viscous dissipation. *International Journal of Heat and Mass Transfer*, 79, 212–222.
- Sheikholeslami, M., & Gorji-Bandpy, M. (2014). Free convection of ferrofluid in a cavity heated from below in the presence of an external magnetic field. *Powder Technology*, 256, 490–498
- Sheikholeslami, M., & Ganji, D. D. (2014a). Numerical investigation for two phase modeling of nanofluid in a rotating system with permeable sheet. *Journal of Molecular Liquids*, 194, 13–19.
- Sheikholeslami, M., & Ganji, D. D. (2014b). Three dimensional heat and mass transfer in a rotating system using nanofluid. *Powder Technology*, 253, 789–796.
- Sheikholeslami, M., & Ganji, D. D. (2014c). Heated permeable stretching surface in a porous medium using Nanofluids. *Journal of Applied Fluid Mechanics*, 7(3), 535–542.
- Sheikholeslami, M., & Ganji, D. D. (2014d). Magnetohydrodynamic flow in a permeable channel filled with nanofluid. *Scientia Iranica B*, 21(1), 203–212.
- Sheikholeslami, M., & Ganji, D. D. (2014e). Ferrohydrodynamic and Magnetohydrodynamic effects on ferrofluid flow and convective heat transfer. *Energy*, 75 (2014) 400–410.
- Sheikholeslami, M., Gorji-Bandpy, M., & Vajravelu, K. (2015a). Lattice Boltzmann Simulation of Magnetohydrodynamic Natural Convection Heat Transfer of Al₂O₃-water Nanofluid in a Horizontal Cylindrical Enclosure with an Inner Triangular Cylinder. *International Journal of Heat and Mass Transfer*, 80, 16–25
- Sheikholeslami, M., Ganji, D. D., Younus J. M., & Ellahi, R. (2015b). Effect of thermal radiation on magnetohydrodynamics nanofluid flow and heat transfer by means of two phase model. *Journal of Magnetism and Magnetic Materials*, 374, 36–43.